

Quantum Breathers in Electron-phonon Systems

W. Z. Wang, A. R. Bishop, J. T. Gammel, and R. N. Silver

Theoretical Division and Center for Nonlinear Studies, Los Alamos National Laboratory, Los Alamos, New Mexico 87545
(October 6, 2018)

Quantum breathers are studied numerically in several electron-phonon coupled finite chain systems, in which the coupling results in intrinsic nonlinearity but with varying degrees of nonadiabaticity. As for quantum nonlinear lattice systems, we find that quantum breathers can exist as eigenstates of the system Hamiltonians. Optical responses are calculated as signatures of these coherent nonlinear excitations. We propose a new type of quantum nonlinear excitation, breather-excitons, which are bound states of breathers and excitons, whose properties are clarified with a minimal exciton-phonon model.

PACS: 63.20.Pw, 63.20.Ls, 63.20.Ry, 71.35.Cc

Much progress has been made toward understanding the physical consequences of nonlinearity over the last decade. In particular, recent developments concerning “breathers” [1] or “intrinsic local modes” (ILM) [2], suggest that energy focusing is prevalent in both classical [2–5] and quantum [6–8] *discrete* nonlinear nonintegrable frameworks. The existence and stability of multiquanta bound states (breathers, ILMs) are now established for a wide variety of discrete classical models with prescribed nonlinearity. Recently, we demonstrated that this property also persists in a discrete quantum nonlinear lattice, and exhibited some distinctive observable signatures in terms of spatial-temporal correlations [8]. However, of more profound concern is the typical origin of effective nonlinearity in quantum systems, namely, through the coupling of two or more fields. Adiabatic slaving of fields usually results in nonlinear Schrödinger models. Realistically, however, nonadiabatic effects must be considered and the influences of nonlinearity and nonadiabaticity are inevitably interrelated. Here we consider examples of electron-phonon (*e-ph*) coupled models frequently used to describe organic and inorganic correlated electronic materials, for which an adiabatic treatment of breathers is inadequate for various physical observables [9]. The interactions of electrons with the lattice and among themselves provide sources of nonlinearity and strongly influence electronic, optical and structural properties. Here, we use numerical approaches restricted to finite chains but without any adiabatic approximation. We find that quantum breathers of *two* types can exist in the *e-ph* systems considered — those near electronic ground states, and photoexcited breathers (termed “breather-excitons” below).

We consider a Holstein-Hubbard (HH) tight-binding model Hamiltonian [10] of an *e-ph* coupled system:

$$H_e = \sum_{i\sigma} -t_0 (c_{i\sigma}^\dagger c_{i+1,\sigma} + \text{H.c.}) \quad (1)$$

$$+ \sum_i U n_{i\uparrow} n_{i\downarrow} + \sum_{i\sigma\sigma'} V n_{i\sigma} n_{i+1\sigma'}$$

$$+ \sum_i \hbar\omega_0 \left(b_i^\dagger b_i + \frac{1}{2} \right) - \sum_{i\sigma} \lambda \left(b_i^\dagger + b_i \right) n_{i\sigma} .$$

Here, $c_{i\sigma}^\dagger$ ($c_{i\sigma}$) and b_i^\dagger (b_i) are the creation (annihilation) operators of electrons and phonons, respectively. t_0 , U and V are the electron kinetic energy, and the on-site and nearest-neighbour Coulomb repulsions. ω_0 is the bare phonon frequency. The form of the *e-ph* coupling (λ term) is that used in the Holstein (H) model [12]. We use models with one electron per site (*i.e.* a $\frac{1}{2}$ -filled band).

Our numerical approach mainly consists of exact diagonalization of Hamiltonian matrices represented in Hilbert spaces defined by appropriately selected basis functions, and the analysis of characteristics of quantum breathers via various dynamic correlation functions. We deal fully with nonadiabaticity and *e-e* correlations; the only approximation is the truncation of the infinite phonon Hilbert space. Because wavefunction information is needed to identify a quantum breather state which is not necessarily low-lying in the complete eigenspectrum, efficient exact diagonalization techniques have been developed to handle large-scale matrices; these are also designed to suit parallel computer architectures [13]. In Fig. 1, we show a typical total density-of-states (DOS) of a HH model, calculated using the kernel polynomial method [14] which has a finite energy resolution. The regions of interest are indicated (see text below Figs. 3 and 5). Comparing to the Hubbard model DOS, we realize that the denser the states the more difficult they are to numerically distinguish, and the higher the numerical efficiency required. Also, since our model systems are finite, it is not easy to eliminate finite-size effects [15]. However, our main results remain valid because the breather excitations of interest here are intrinsically of finite size. There are also many realistic material contexts which are of finite-size (*e.g.* conjugated oligomers).

The eigen-energies of the system (1) are shown in Figs. 2 and 3 for 6-site Holstein, and HH models, respectively. The results in Fig. 2 were obtained using a basis set of Debye phonons and Bloch electron functions, while Fig. 3 results use Einstein phonons and Wannier func-

tions. The degrees of softening of the $k = \pi$ mode (Kohn anomaly) indicate that the systems in Figs. 2(a) and 3 are weakly e -ph coupled, whereas that in Fig. 2(b) is more strongly coupled. The phonon dispersion is caused by effective nonlinear ph-ph coupling via the e -ph coupling. Because of discrete translational invariance, direct examination of the wavefunction amplitudes and single phonon operator expectation values do not reveal the presence of quantum breathers [8]. Rather, we examine various static and dynamic correlation functions of lattice displacements, including: $U_j^k(t) = \sum_i \langle k | u_i(0) u_j(t) | k \rangle$, where u_i is the phonon displacement operator. The static correlation functions ($t=0$) probe the spatial localization in a given eigenstate, while the dynamic counterparts probe the temporal coherence. These two properties are the distinguishing characteristics of quantum breathers [1,2]. The correlation functions $U_j^k(t)$, as in Fig. 4, show that there indeed exists a band of particle-like states in each of the above examples, and that these states possess short but finite spatial and temporal correlations, whereas all other states are extended [16]. A typical case is shown in Fig. 2(b), where the particle-like band possesses a large binding energy separating it from the continuum bands above, and the anharmonicity and corresponding localization are strong (the correlation length is approximately 3 lattice constants, see Fig. 4) [10].

The existence and properties of quantum breathers depend not only on the effective nonlinear ph-ph coupling (as in [8]) but also on the nonadiabaticity (here, controlled by the ratio $\hbar\omega_0/t_0$). We find that the stronger the e -ph coupling and the adiabaticity, the more easily quantum breathers form [16]. Furthermore, these breather states can survive strong e - e correlations (Fig. 3), although we find that in the lowest part of the excitation spectrum strong e - e correlations tend to induce extended magnetic excitations [16]. We will see below, however, that strong e - e correlations do not necessarily destroy short-correlation length breathers in other spectral regions.

To identify physical consequences of the breather excitations, we study the first-order optical response function which can be measured in one-photon experiments. Fig. 5 shows the zero-temperature infrared and electronic optical absorptions of a HH system. Within this nonadiabatic approach, we account for all the electronic and phonon polarizabilities within one photon perturbations. This is a step toward understanding accumulating experimental results in ultra-fast time-resolved (nonadiabatic) and nonequilibrium measurements [17]. First, we observe that in the infrared region, several prominent peaks directly indicate the anharmonicity, including multiphonon side-bands. Comparing to Fig. 3, the contribution to the infrared absorption from the breather states (marked “ b ”) has comparable intensity to that from surrounding extended states. Second, below the main absorption peak (marked “*exciton*”), there exist a series of spectral

features which cannot be explained in an adiabatic description. To understand their origin, we added small amounts of disorder in the electron or phonon degrees of freedom (*e.g.*, the parameters U or $\hbar\omega_0$). We found that only phonon disorder changes the spectral features near the “*exciton*” edge [16], indicating their phonon origin. Third, in addition to the rich structure in the region of electronic absorption, we observe a series of bands between the “*exciton*” edge and the “*continuum*” bands. Among them, we notice one band (“ b - e ”) whose position and intensity relative to the other phonon sidebands does not change under the perturbation of phonon disorder [16]. This indicates that this particular band is due to some a relatively stable excited configurations which are more localized. This evidence suggests a possible new type of bound state which is higher in energy than the lowest excitons and more localized than the nearby states — we will term these *breather-excitons*. Below we show that they possess some of the characteristics of the “ground state” quantum breathers identified in the low-lying part of the eigenspectrum [Fig. 3].

Physical intuition suggests the possibility of a bound state of excitons and breathers, *i.e.* a hot (dressed) exciton or a photoexcited breather. Excitons exist primarily as electron-hole pairs bound by both the Coulomb interactions and e -ph coupling. The latter factor slows down the exciton motion and tends to dress the exciton with phonons and breathers. e - e correlations provide another energy region from which the breather can be excited, and contribute additional nonlinearity enhancing the breather formation. Furthermore, with the excited oscillating dipole moments inside the breather-exciton bound states, they will strongly absorb photons, as an electronic exciton does.

To support the above arguments [18], we introduce a minimal exciton-phonon model, describing an electron and hole interacting with each other and with phonons:

$$\begin{aligned}
H = & \sum_i -t_e \left(e_i^\dagger e_{i+1} + \text{H.c.} \right) + \sum_i \epsilon_e e_i^\dagger e_i \\
& \sum_i -t_h \left(h_i^\dagger h_{i+1} + \text{H.c.} \right) - \sum_i \epsilon_h h_i^\dagger h_i \\
& + \sum_{i,j} V(i-j) e_i^\dagger e_i h_j^\dagger h_j \\
& - \sum_i \lambda_e \left(b_i^\dagger + b_i \right) e_i^\dagger e_i - \sum_i \lambda_h \left(b_i^\dagger + b_i \right) h_i^\dagger h_i \\
& + \sum_i \hbar\omega_0 \left(b_i^\dagger b_i + \frac{1}{2} \right), \tag{2}
\end{aligned}$$

with $V(i-j) = -U$ (as $i = j$); $-V$ (as $|i-j| = 1$); and 0 (otherwise). e_i^\dagger (e_i) and h_i^\dagger (h_i) are creation (annihilation) operators for the electron and hole, respectively. $t_{e(h)}$, $\epsilon_{e(h)}$, $V(i-j)$ and $\lambda_{e(h)}$ are the electron (hole) hopping integrals, on-site energies, electron-hole attractions and $e(h)$ -ph couplings strengths, respec-

tively [19]. Fig. 6 shows the low-lying part of the eigen-spectrum, corresponding to the “exciton” region in Fig. 5. The lowest band corresponds to the lowest exciton states in Fig. 5 and shows dispersion. They are excitons dressed by a static lattice distortion of condensed phonons. The breather-exciton states are also strongly localized, but dressed with a dynamic phonon wavepacket (weak dispersion) and exhibiting more coherent internal motions. (We speculate that the excitonic internal frequency resonantly traps a breather.) The remaining states are e - h pairs coupled to extended anharmonic phonons. Breather-excitons are more polarized than the ground state breathers, leading to the stronger optical absorption seen in Fig. 5.

In summary, this study is an important extension of previous investigation of quantum breathers in nonlinear lattices [8]. It demonstrates their existence in more general e -ph systems where nonlinearity is self-consistently generated by the e -ph (and e - e) coupling rather than being inserted by hand. Thus the combined influences of nonadiabaticity and nonlinearity are incorporated. Clear features from breathers are found in optical properties. The concept of *breather-exciton* states was proposed and demonstrated for a simplified exciton-phonon model without any adiabatic approximations. Investigations are underway [20] to correlate our findings with nonlinear optics and time-resolved spectroscopy, including the competing timescales associated with exciton formation, excitonic self-trapping, and breather-exciton formation, as functions of nonlinearity and nonadiabaticity [16].

We are grateful to M. I. Salkola and J. Zang for many useful discussions and previous collaborations. We also thank S. R. White, C. L. Zhang, Z. V. Vardeny, L. Yu and Z. B. Su for helpful discussions. This computation was performed at the CM-5 of ACL and the Sun UE-4000 of T-11 at Los Alamos National Laboratory. The research is supported by the U.S. Department of Energy.

-
- [1] See, *e.g.*, A. R. Bishop, *et al.*, *Physica* **D1**, 1 (1980).
[2] See, a recent review of S. Flach and C. R. Willis, *Phys. Reports*, in press (1997).
[3] A. J. Sievers and J. B. Page, in *Dynamic Properties of Solids VII*, p. 137, ed. G. K. Horton and A. A. Maradudin (Elsevier, Amsterdam, 1995).
[4] G. P. Tsironis and A. Aubry, *Phys. Rev. Lett.* **77**, 4776 (1996).
[5] S. Flach, *et al.*, *Phys. Rev. Lett.* **78**, 1207 (1997).
[6] *e.g.*, R. Jackiw, *Rev. Mod. Phys.* **49**, 681 (1977).
[7] S. Takeno, *J. Phys. Soc. Japan* **59**, 3127 (1990); A. C. Scott, *et al.*, *Physica* **D78**, 194 (1994); A. Aubry, *Physica* **D103**, 201 (1997).
[8] W. Z. Wang, *et al.*, *Phys. Rev. Lett.* **76**, 3598 (1996).

- [9] *e.g.*, B. Horovitz, *et al.*, *Phys. Rev.* **B40**, 1240 (1989).
[10] We have obtained similar results for the SSH model [11,16].
[11] W. P. Su, *et al.*, *Phys. Rev. Lett.* **42**, 1698 (1979).
[12] T. D. Holstein, *Ann. Phys. (N.Y.)* **8**, 325 (1959).
[13] W. Z. Wang, Ph.D Thesis (unpublished).
[14] R. N. Silver and H. Röder, *J. Mod. Phys.* **B5**, 735 (1994).
[15] A feasible first step has recently been taken to study finite-size effects. C. L. Zhang and S. R. White, private communication.
[16] W. Z. Wang, *et al.*, (unpublished).
[17] *e.g.*, M. Ozaki, *et al.*, *Phys. Rev. Lett.* **79**, 1762 (1997).
[18] Because the DOS in the “exciton” region is too high to apply any available spectral transformation methods, we are currently unable to accurately solve for the eigenstates in this region for the full HH model [cf. Fig. 1].
[19] Only simplified $e(h)$ -ph and e - h interactions are retained in Eq. (2) because no exact mapping is available between an effective exciton-phonon model and the original half-filled HH model.
[20] W. Z. Wang, Z. G. Shuai, A. B. Saxena and A. R. Bishop, unpublished (1997).

FIG. 1. Total DOS of a 6-site Holstein-Hubbard chain with $t_0 = 1.00$, $\omega = 0.40$, $\lambda = 0.31$, $U = 8.10$, $V = 1.11$, $M_{\text{ph}} = 4$, and $\mathcal{M} = 1\,638\,400$. (M_{ph} and \mathcal{M} stand for phonon truncation and the total dimension of the matrix.) The inset shows the DOS over the full energy range, with the corresponding pure Hubbard model (gray line) results for comparison.

FIG. 2. Eigenspectrum (low-lying sector) of a 6-site Holstein chain with $t_0=1.00$, $\omega=0.4$, $U=V=0.00$ and (a) $\lambda = 0.31$, $M_{\text{ph}}(k = \pm\frac{\pi}{3}, \pm\frac{2\pi}{3}) = 5$, $M_{\text{ph}}(k = \pi) = 6$, $M_{\text{ph}}(k = 0) = 1$, $\mathcal{M} = 1\,500\,000$; (b) $\lambda = 0.61$, $M_{\text{ph}}(k = \pm\frac{\pi}{3}, \pm\frac{2\pi}{3}) = 6$, $M_{\text{ph}}(k = \pi) = 10$, $M_{\text{ph}}(k = 0) = 1$, $\mathcal{M} = 5\,184\,000$. The breather states are labeled with solid triangles, and the remaining ones with open triangles. The ground state energy has been subtracted from E_k .

FIG. 3. Eigenspectrum of the 6-site Holstein-Hubbard chain in Fig. 1. The notation is as in Fig. 2. The ground state energy is $4.14t_0$

FIG. 4. The spatial correlation function $U_j^k(0)$ of the system in Fig. 2(b). The solid line is for a breather state (labeled B in Fig. 2(b)), while the gray line is for an extended state (E).

FIG. 5. The zero-temperature infrared and electronic optical absorptions of the 6-site Holstein-Hubbard system in Fig. 3 (solid line) and the related 6-site Hubbard model with $t_0 = 1.00$, $U = 8.10$, $V = 1.11$ (gray line). All spectra are broadened by a Lorentzian of width 0.005.

FIG. 6. Eigenspectrum (low-lying sector) of the 6-site minimal exciton-phonon model (see text) with $t_e = 1.00$, $t_h = 0.67$, $\epsilon_e = 4.00$, $\epsilon_h = -4.00$, $\omega_0 = 0.15$, $U = 18.0$, $V = 2.75$, $\lambda_e = 0.87$, $\epsilon_h = -0.27$. $M_{\text{ph}} = 6$, $\mathcal{M} = 1\,679\,616$. The breather-exciton states are labeled with solid triangles, the dressed excitons with diamonds, and the remaining ones with open triangles. The ground state energy has been subtracted from E_k .

Figures in “Quantum Breathers in Electron-phonon Systems” by
W. Z. Wang *et al.*, November 1997.

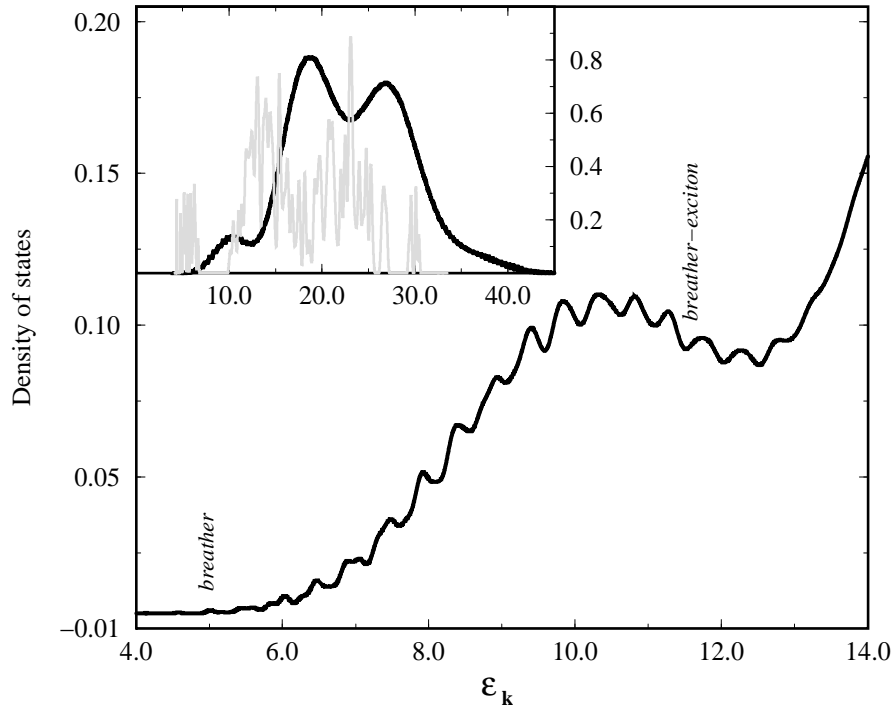


FIG. 1. Total DOS of a 6-site Holstein-Hubbard chain with $t_0 = 1.00$, $\omega = 0.40$, $\lambda = 0.31$, $U = 8.10$, $V = 1.11$, $M_{\text{ph}} = 4$, and $\mathcal{M} = 1638400$. (M_{ph} and \mathcal{M} stand for phonon truncation and the total dimension of the matrix.) The inset shows the DOS over the full energy range, with the corresponding pure Hubbard model (gray line) results for comparison

Figures in “Quantum Breathers in Electron-phonon Systems” by
W. Z. Wang *et al.*, November 1997.

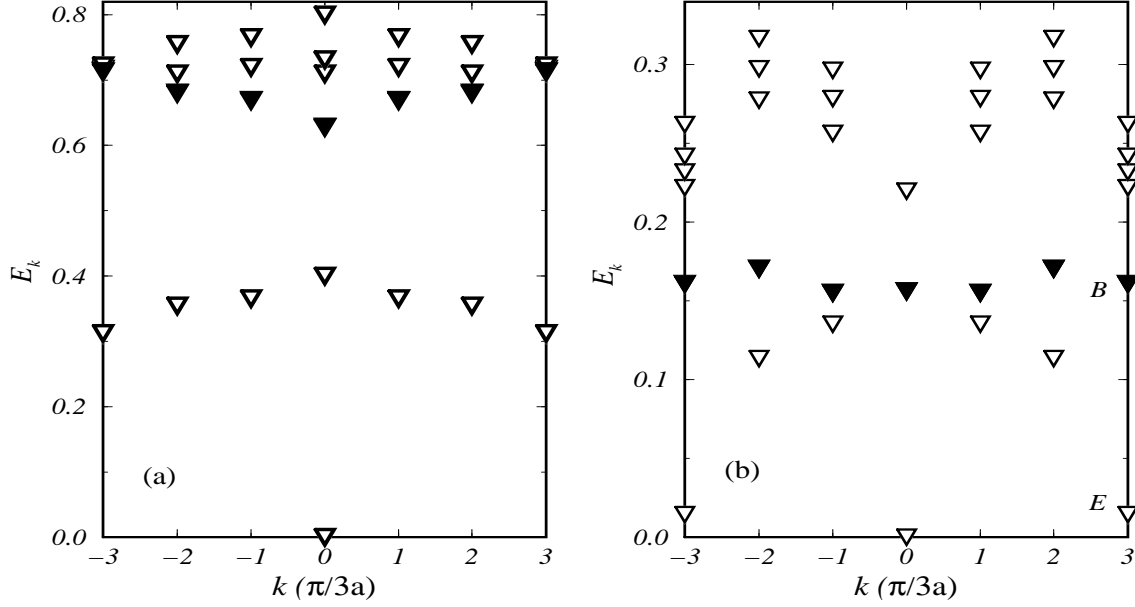


FIG. 2. Eigenspectrum (low-lying sector) of a 6-site Holstein chain with $t_0=1.00$, $\omega=0.4$, $U=V=0.00$ and (a) $\lambda = 0.31$, $M_{\text{ph}}(k = \pm\frac{\pi}{3}, \pm\frac{2\pi}{3}) = 5$, $M_{\text{ph}}(k = \pi) = 6$, $M_{\text{ph}}(k = 0) = 1$, $\mathcal{M} = 1\,500\,000$; (b) $\lambda = 0.61$, $M_{\text{ph}}(k = \pm\frac{\pi}{3}, \pm\frac{2\pi}{3}) = 6$, $M_{\text{ph}}(k = \pi) = 10$, $M_{\text{ph}}(k = 0) = 1$, $\mathcal{M} = 5\,184\,000$. The breather states are labeled with solid triangles, and the remaining ones with open triangles. The ground state energy has been subtracted from E_k .

Figures in “Quantum Breathers in Electron-phonon Systems” by
W. Z. Wang *et al.*, November 1997.

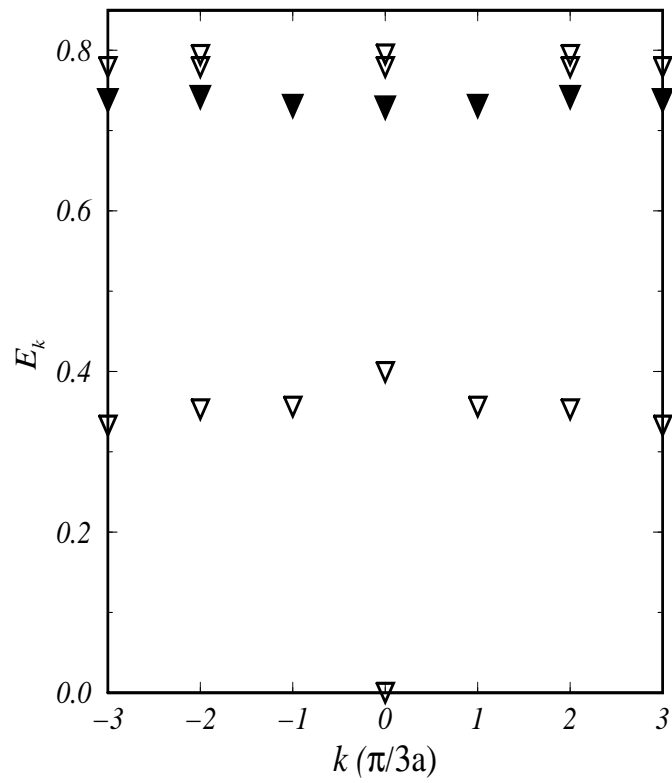


FIG. 3. Eigenspectrum of the 6-site Holstein-Hubbard chain in Fig. 1. The notation is as in Fig. 2. The ground state energy is $4.14t_0$

Figures in “Quantum Breathers in Electron-phonon Systems” by
W. Z. Wang *et al.*, November 1997.

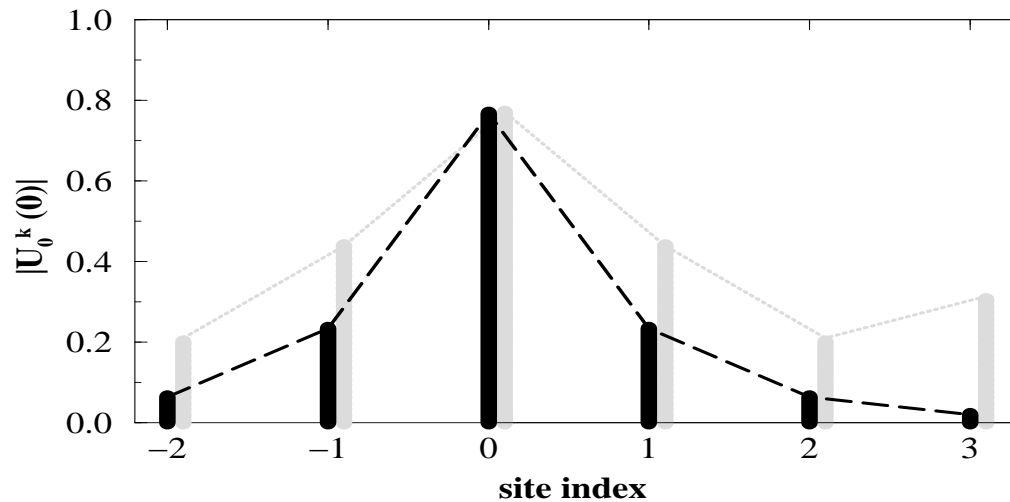


FIG. 4. The spatial correlation function $U_j^k(0)$ of the system in Fig. 2(b). The solid line is for a breather state (labeled B in Fig. 2(b)), while the gray line is for an extended state (E).

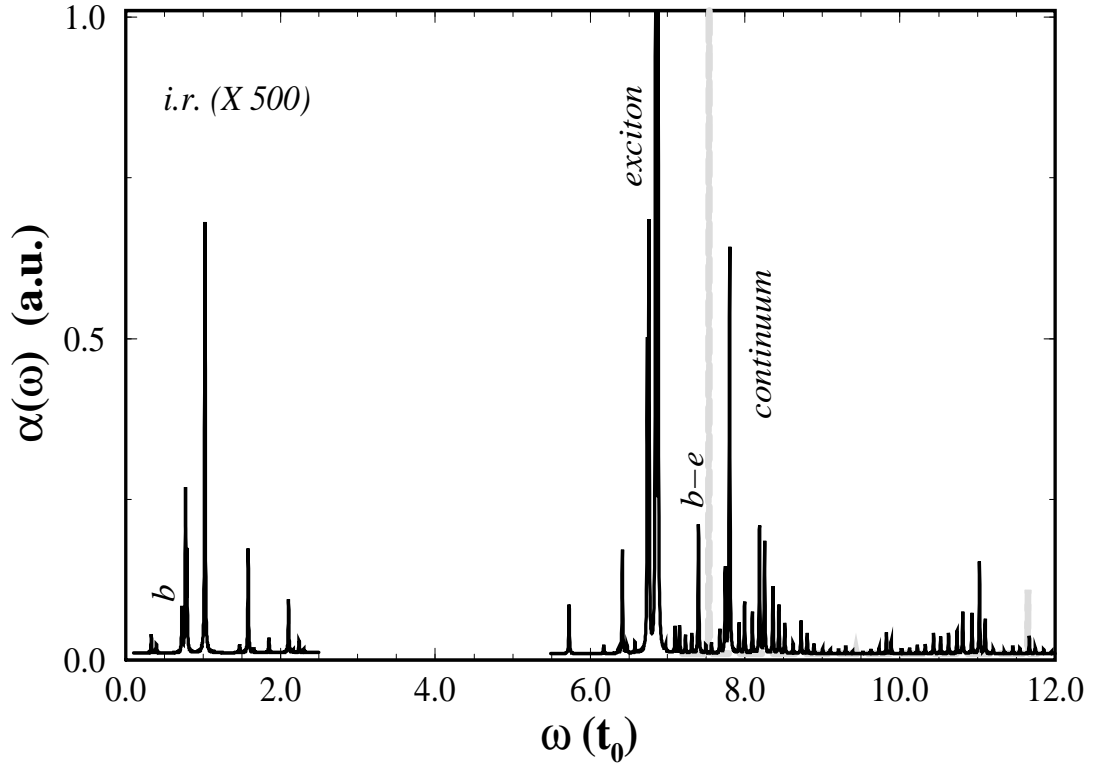


FIG. 5. The zero-temperature infrared and electronic optical absorptions of the 6-site Holstein-Hubbard system in Fig. 3 (solid line) and the related 6-site Hubbard model with $t_0 = 1.00$, $U = 8.10$, $V = 1.11$ (gray line). All spectra are broadened by a Lorentzian of width 0.005.

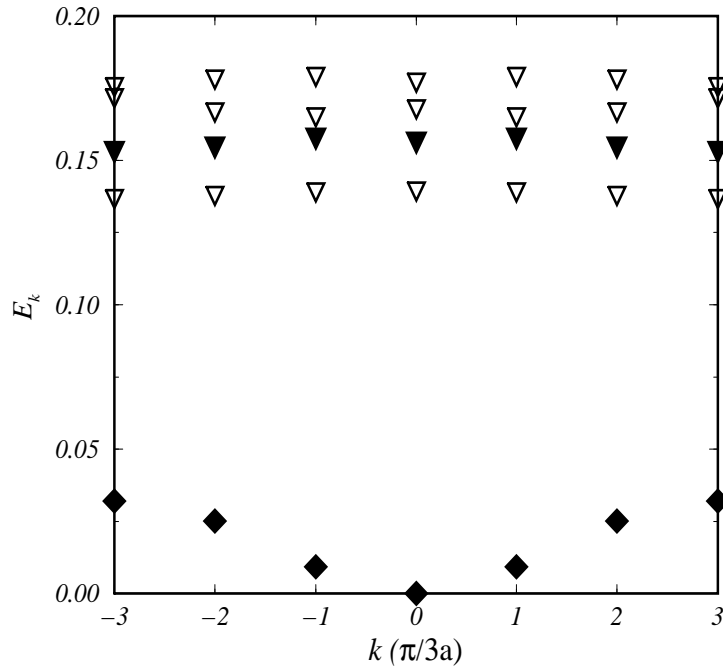


FIG. 6. Eigenspectrum (low-lying sector) of the 6-site minimal exciton-phonon model (see text) with $t_e = 1.00$, $t_h = 0.67$, $\epsilon_e = 4.00$, $\epsilon_h = -4.00$, $\omega_0 = 0.15$, $U = 18.0$, $V = 2.75$, $\lambda_e = 0.87$, $\epsilon_h = -0.27$. $M_{\text{ph}} = 6$, $\mathcal{M} = 1\,679\,616$. The breather-exciton states are labeled with solid triangles, the dressed excitons with diamonds, and the remaining ones with open triangles. The ground state energy has been subtracted from E_k .